

Stable positron acceleration via laser-augmented blowouts in two-column plasma structures

Lars Reichwein* and Alexander Pukhov

Institut für Theoretische Physik I, Heinrich-Heine-Universität Düsseldorf, 40225 Düsseldorf, Germany

Anton Golovanov and Igor Yu. Kostyukov

Institute of Applied Physics RAS, 603950 Nizhny Novgorod, Russia

(Dated: May 16, 2022)

We propose a setup for efficient positron acceleration consisting of an electron driver and a laser pulse creating a two-fold plasma column structure. The resulting wakefield is capable of stably accelerating positron bunches over long distances even when evolution of the driver is considered. The scheme is studied by means of particle-in-cell simulations. Further, the analytical expression for the accelerating and focusing fields are obtained, showing the equilibrium lines along which the witness bunch is accelerated.

The efficient acceleration of positrons is of great interest for fundamental physics, especially for the electron-positron colliders [1]. In the field of accelerator physics, laser-plasma based schemes have specifically grown in interest over the last few decades, as the higher achievable field strengths compared to conventional accelerators allow for higher energies over shorter acceleration distances.

Acceleration in plasma wakefield can be accomplished either with a driving laser pulse [2, 3] or a driving particle bunch [4]. For the laser-driven setup, a so-called bubble can be excited for a normalized laser vector potential $a_0 > 1$, while for the electron-bunch driven setup a sufficiently narrow and high-density bunch has to be used. In both cases, the driver pushes out electrons in the direction transverse to its propagation leaving behind an electronic cavity (“bubble”). Electrons can be injected into the back part of the bubble via several mechanisms, such as self-injection [5], ionization injection [6], or density down-ramp injection [7]. For appropriately chosen laser-plasma parameters, the excited bubble exhibits uniform accelerating fields that propagate with a velocity close to the speed of light c , which allows for the acceleration of mono-energetic electron bunches [8]. Utilizing more complicated setups like Trojan horse injection [9], emittances in the order of nm rad and energy spreads in the 0.1% range were achieved. Currently realizable in the case of homogeneous plasma are electron bunches of up to 8 GeV [10].

In the case of positrons, wakefield acceleration proves to be a more difficult challenge: the accelerating and focussing region for positrons in non-linear wakefields is comparatively small. Thus, more advanced setups are necessary. One of the proposed setups utilizes donut-shaped electron bunches as drivers [11]. Other setups use drive bunches consisting of positrons or hollow plasma targets [12–14]. While these schemes improve on the extent of the accelerating region, they still pose problems

either in experimental feasibility or stability.

In a recent work [15], Diederichs *et al.* have proposed a setup using a laser-ionized plasma column of finite radius that is penetrated by an electron driver. Such columns have been shown to be experimentally realizable for radii in the range of several tens of micrometers and peak densities of ca. 10^{17} cm^{-3} [16, 17]. Due to the column’s finite radius, the field structure is different from the case of wakefields in homogeneous plasma. As observed there, the finite plasma column benefits the acceleration of Gaussian positron bunches. What remains critical, however, is the evolution of the electron driver which commonly leads to negative effects when accelerating positrons. A follow-up study of beam loading in this regime which incorporated an algorithm for optimizing the bunch profile was presented in [18]. Still, in experiments the effects of beam evolution are likely to negatively influence the efficient acceleration over long distances.

In this letter, we present a novel laser-augmented blowout (LAB) scheme for the stable acceleration of positrons over distances of tens of centimeters. An electron drive bunch ionizes a narrow column of hydrogen gas and excites a wakefield. A separate laser pulse ionizes a wider column behind the driver. This creates a region beneficial for the acceleration of positron rings (Fig. 1). This ring bunch geometry further has the advantage that it will avoid beamstrahlung similarly to flat beams proposed for high-energy colliders like CLIC and is still suitable for acceleration in plasma much like round bunches [19]. We will first present our scheme in terms of particle-in-cell (PIC) simulations. Further, the accelerating and focusing fields are derived analytically. The field structure exhibits equilibrium lines along which the positron ring is located. Finally, the emittance and the energy spectrum of the witness bunch are studied. Matching the positron ring according to the setup parameters yields a reduction of the emittance growth.

For our simulations we use the quasistatic PIC code QV3D [20]. In our presented example (Fig. 2), our simulation box has dimensions $16 \times 20 \times 20k_p^{-3}$ with grid size

* lars.reichwein@hhu.de

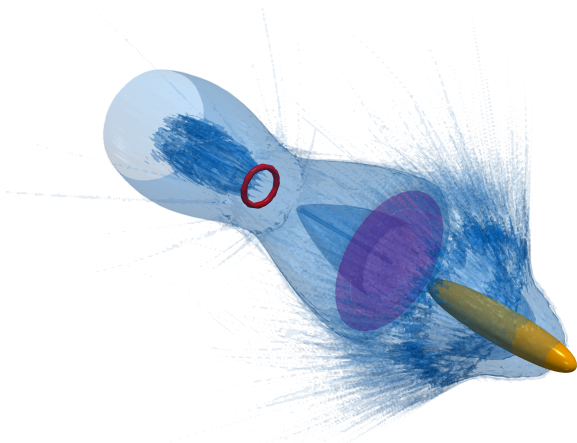


Figure 1. Three-dimensional rendering of the LAB scheme. The electron driver (orange) pushes the electrons (blue) out in the transverse direction and the second column is ionized by the laser pulse (magenta). The positron ring (red) is located in the vicinity of the region with the highest electron density.

$h_x = h_y = h_z = 0.05k_p^{-1}$ where $k_p = 2\pi/\lambda_p$ is the plasma wave number ($\lambda_p = 75 \times 10^{-4}$ cm).

The box is filled with initially ionized hydrogen gas with a density of $n_0 = 2 \times 10^{17}$ cm $^{-3}$. A Gaussian-shaped electron driver with dimensions $\sigma_z = 12$ μ m (z being the direction of propagation) and $\sigma_x = \sigma_y = 2.4$ μ m performs the initial ionization. It has a peak density of $20n_0$ and the initial momentum of the electrons is $p_z = 10^4 m_e c$ with 5% longitudinal spread (m_e being the electron rest mass). The driver excites a wakefield whose fields exhibit a different structure compared to the case of homogeneous plasma (we will see this in the analytic theory later on in more detail).

A short ($\tau_0 = 4.5$ fs) laser pulse ionizes a second, wider column. Since we want to consider acceleration up to $2 \times 10^4 T_0$ we need a corresponding Rayleigh length, meaning that our focal spot size should be $w_0 \approx 125$ μ m. Such laser pulses could be created at the LWS-20 laser which has 16 TW peak power and 70–75 mJ pulse energy [21]. Different radii may also be used: Presented in Fig. 2 we show the setup for $w_0 = 17$ μ m for better visibility of the parameters that we will use for the analytic discussion.

We observe that, in the region right behind the electron driver, fields reminiscent of typical blowout structures in homogeneous plasma can be seen. Since only a narrow part of the total gas in the simulation box is ionized, the fields extend over a greater distance leading to a slightly modified blowout structure. Specifically in the region $\xi = (5 - 7)k_p^{-1}$, the diagonal white lines in the structure of the focusing force $E_r - B_\varphi$ prove to be beneficial for positron acceleration. Further, a look at the accelerating field E_z shows that along these lines, the positrons will experience a maximum accelerating field from the subsequent blowout structure.

Thus, we place the positron ring accordingly (cf. Fig. 1). Its density is varied in the range of $1n_0$ to $80n_0$ for the

different performed simulations. Its initial radius is 4.8 μ m and the positrons have an initial momentum of $p_z = 10^4 m_e c$. Such positron rings could be created in a similar fashion to hollow electron bunches via the utilization of Laguerre-Gaussian laser pulses [22, 23].

As we will now also analytically verify, this location corresponds to an equilibrium line where the radial electric field E_r vanishes and, at the same time, the highest accelerating field for that transverse position is reached. A strongly mismatched positron beam would lead to the loss of positrons and worse emittance.

To obtain the structure of the electromagnetic fields of the LAB scheme analytically, we proceed in a similar fashion to the approach in [24] using the following plasma setup in the quasi-static approximation

$$\rho_e(0, r) = \begin{cases} -1, & r_1 < r < r_2 \\ 0, & \text{else} \end{cases}, \quad (1)$$

$$\rho_i(\xi, r) = \begin{cases} 1, & r < r_2 \\ 0, & \text{else} \end{cases}, \quad (2)$$

where $\xi = t - z$ denotes the co-moving coordinate and r_1, r_2 indicate the column radii (cmp. Fig. 2). The position $\xi = 0$ corresponds to the point where the laser pulse ionizes the plasma ring $r_1 < r < r_2$, and we neglect the contribution of electrons ionized and expelled by the electron driver (assuming they are expelled to $r > r_2$). Ions are considered immobile, but plasma electrons begin to converge to the axis r due to the action of the radial electric field E_r from the ion column, which can be calculated as

$$E_r(\xi, r) = \frac{1}{r} \int_0^r [\rho_i(\xi, r') + \rho_e(\xi, r')] r' dr'. \quad (3)$$

Here, we assume that the motion of the electrons is predominantly radial and neglect the influence of the longitudinal field E_z on them, so they do not generate longitudinal current j_z and azimuthal magnetic field B_φ . We also assume that the motion is non-relativistic and that electron trajectories never cross, so the motion of the electron with the initial coordinate r_0 is always affected only by the Coulomb field of the electrons with initial coordinates smaller than r_0 , and we get

$$\frac{d^2 r}{d\xi^2} = -E_r = -\frac{r}{2} + \frac{r_0^2 - r_1^2}{2r}, \quad (4)$$

where the first term is the Coulomb attraction from the ions, and the second term is the Coulomb repulsion from the inner electrons. If we further assume that $|r - r_0| \ll r_0$ and $r_0 \gg r_1$, we obtain

$$r = r_0 - \frac{r_1^2}{2r_0} (1 - \cos \xi). \quad (5)$$

All electrons oscillate with the same period equal to the plasma wavelength in this solution. As the oscillation amplitude decreases with r_0 , trajectory crossing never

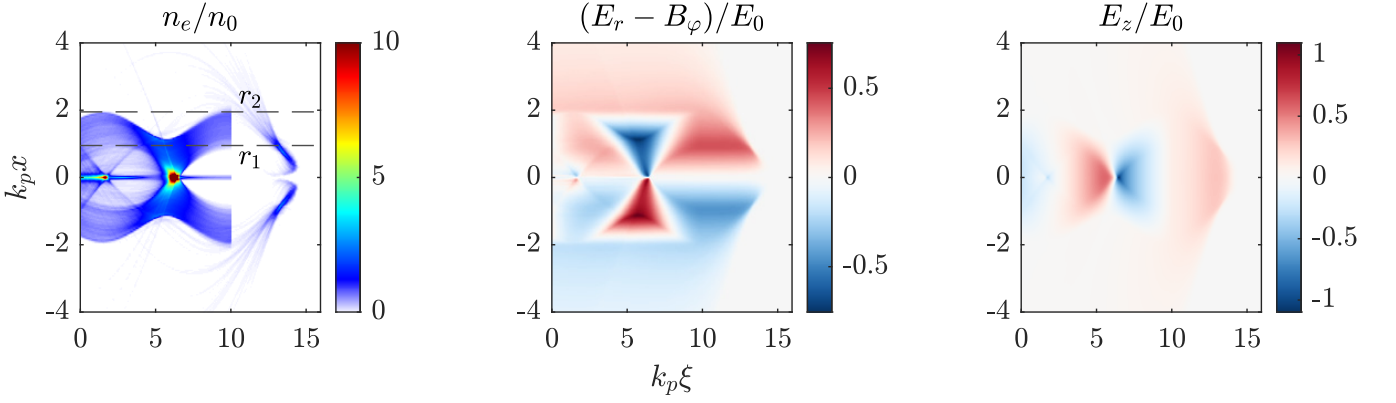


Figure 2. PIC simulation results for the LAB scheme with the $w_0 = 17 \mu\text{m}$ laser pulse. (a) The electron density (clipped at $n = 10n_0$ for better visibility) shows the fork-like structure. Around its area of highest density, the positron ring is located ($\xi \approx 6.1k_p^{-1}$, $x \approx \pm 0.4k_p^{-1}$). The values r_1 and r_2 denote the radii used in the analytical derivation of the fields. As seen in (b), this location of the positrons coincides with the equilibrium line for the focusing force as well as the area where the accelerating gradient of E_z is the largest (c).

happens for this solution. Let us now assume that this solution is valid for all electrons with initial coordinates in the interval $[r_1, r_2]$, i.e. for a given ξ all electrons are located between

$$r_{\min} = \frac{r_1}{2}(1 + \cos \xi), \quad r_{\max} = r_2 - \frac{r_1^2}{2r_2}(1 - \cos \xi). \quad (6)$$

Knowing all trajectories allows us to calculate the density

distribution and thus the transverse electric field

$$E_r(\xi, r) = \begin{cases} \frac{r}{2}, & r < r_{\min}(\xi) \\ \frac{r}{2} - \frac{r_0^2(\xi, r) - r_1^2}{2r}, & r_{\min} < r < r_{\max} \\ \frac{r}{2} - \frac{r_2^2 - r_1^2}{2r}, & r_{\max}(\xi) < r < r_2 \\ \frac{r_1}{2r}, & r > r_2. \end{cases} \quad (7)$$

Here we introduced

$$r_0(\xi, r) = \frac{r + \sqrt{r^2 + 2r_1^2(1 - \cos \xi)}}{2}, \quad (8)$$

which is the electron's initial coordinate r_0 expressed through its current radial coordinate r . For $r < r_{\min}$ we observe the electric field typical for long ion channels [25, 26]. Outside of the plasma column width, $r > r_2$, we see that $E_r \propto r^{-1}$, which will be valid until electrons expelled from $r < r_1$ begin to contribute to E_r .

In turn, the accelerating field is calculated from the Panofsky–Wenzel theorem [27], $\partial E_z / \partial r = \partial E_r / \partial \xi$,

$$E_z = \begin{cases} E_{z,0}(\xi) - \frac{r_1^2 \sin \xi}{4} \ln \left[\sqrt{\frac{r_2(r_1 - r_{\min})}{r_1(r_2 - r_{\max})}} \frac{r_{\max}}{r_{\min}} \right], & r < r_{\min}(\xi) \\ E_{z,0}(\xi) - \frac{r_1^2 \sin \xi}{4} \ln \left[\sqrt{\frac{r_2(r_0 - r)}{r_0(r_2 - r_{\max})}} \frac{r_{\max}}{r} \right], & r_{\min}(\xi) < r < r_{\max}(\xi) \\ E_{z,0}(\xi), & r > r_{\max}(\xi), \end{cases} \quad (9)$$

where $E_{z,0}$ is the additional longitudinal field created by the electrons expelled by the driver. For simplicity, we assume that $E_{z,0} = 0$. These fields now allow us to calculate the aforementioned equilibrium lines along which the positron ring will be located. First, we find the line where $E_r = 0$. Using equation (7) and incorporating the

restrictions that r_2 imposes on ξ , we obtain

$$r_{\text{eq}} = r_1 \frac{1 + \cos \xi}{2\sqrt{-\cos \xi}}. \quad (10)$$

If we linearize E_r along this line, we will see that it is focussing for positrons, thus making it possible to confine positrons in the transverse direction along this line.

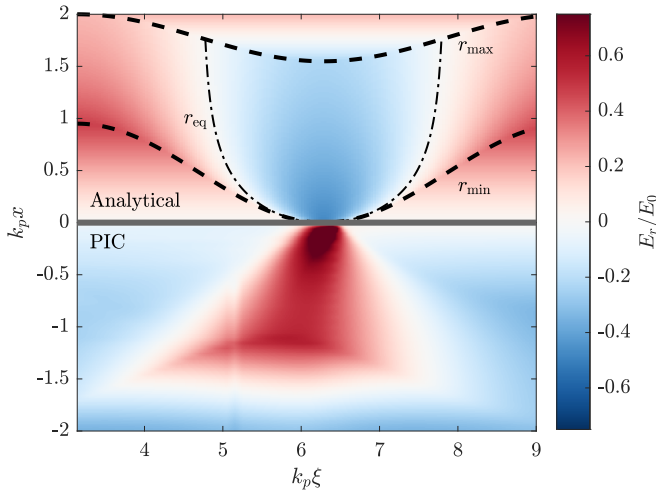


Figure 3. Comparison of the analytical expression and the simulations results for the structure of E_r . The dashed lines denote the lines r_{\min} and r_{\max} from eq. (6) that parameterize the borders of the different field regions and the dashed-dotted line denotes the equilibrium line r_{eq} along which the positron ring can be accelerated from eq. (10).

The positrons are specifically accelerated where E_z gets maximized. By putting our solution for r_{eq} into the expression for E_z , we get

$$E_{z,\text{eq}} = -\frac{r_1^2 \sin \xi}{4} \ln \left[\frac{-4 \cos \xi}{1 - \cos^2 \xi} \frac{r_2^2}{r_1^2} - \frac{2 \cos \xi}{1 + \cos \xi} \right]. \quad (11)$$

This distribution is symmetrical around $\xi = \pi$. As we can see from the equations above, the equilibrium line itself does not depend on r_2 , but $E_{z,\text{eq}}$ does. If we want to achieve the highest possible accelerating gradient, it is therefore beneficial to increase r_2 . However, the scaling $E_{z,\text{eq}} \propto \ln(r_2/r_1)$ is comparatively weak.

A comparison of our analytical result with the simulation can be seen in Fig. 3. The analytical structure qualitatively agrees very well with the numerical result: Along the dashed-dotted equilibrium line $r_{\text{eq}}(\xi)$ the positron ring can be accelerated. This location coincides with the largest possible E_z for that transverse position. The field structure in the simulations is not symmetric, however, because of the limit of applicability of the assumptions we made, as the real oscillation period of electrons depends on their initial radial position.

For the beam quality, we consider the normalized rms emittance $\epsilon_x = \sqrt{\langle x^2 \rangle \langle p_x^2 \rangle - \langle x p_x \rangle^2} / m_e c$ (and accordingly also in y -direction). Here, x denotes the displacement of the particles in x -direction and p_x the corresponding momentum component. The operator $\langle \cdot \rangle$ is the second central moment of the particle distribution. As shown in Fig. 4, the emittance increases over the course of the simulation. In the beginning, both ϵ_x and ϵ_y grow similarly. After roughly $10^4 T_0$, the difference in their slope becomes more pronounced, most likely due to the presence of plasma. Towards the end, the slope flattens and a “saturation point” of around

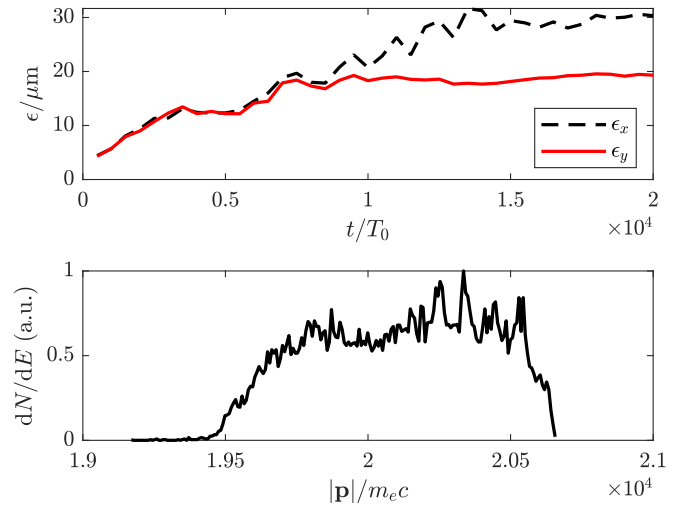


Figure 4. The evolution of the normalized rms emittance (top) for a positron ring with $10n_0$. The emittance starts to increase but reaches a plateau towards the simulation end. The bottom frame shows the final energy spectrum of the accelerated positron bunch after $2 \times 10^4 T_0$.

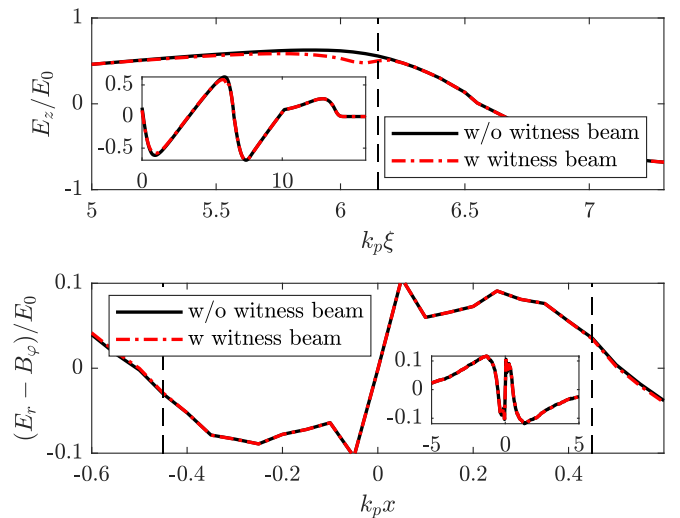


Figure 5. Lineout plots for the accelerating electric field (top) and the transverse force (bottom), both for the cases with witness beam (here, $10n_0$) and without. The lineouts are taken at the initial position of the position ring (further denoted by the dashed lines). The insets show their larger scale behaviour of the fields.

$\epsilon_x \approx 30 \mu\text{m}$, $\epsilon_y \approx 20 \mu\text{m}$ is reached. Strong mismatching of the positron beam size with the plasma setup leads, as mentioned earlier, to the defocusing and loss of positrons and subsequently to higher emittance.

The accelerating and focusing fields that are prominent at the position of the ring are shown in Figure 5. We observe an accelerating gradient of $E_z \approx 38 \text{ GV/m}$. The structure typical for the accelerating field E_z of the wakefield can be observed. Adjusting the density and the dimensions of the positron beam leads to flattening of the

accelerating field in the surrounding region.

In total, we accelerate roughly 15 pC of positrons in the case of a ring with initial density $10n_0$ (with $n_{\text{driver}} \approx 670$ pC). For our presented simulation, the mean positron energy is in the range of 10 GeV after acceleration over a length of 24 cm. As we observe in Fig. 4, the final energy spread of the accelerated positrons is around 1.5%. Increasing the initial density of the positron ring, we are able to accelerate ca. 120 pC with the same setup. For even higher initial densities, the beam loading leads to a loss of additional charge, and the emittance and the energy spectrum deteriorate accordingly.

In conclusion, we have shown that the laser-augmented blowout (LAB) scheme allows for the efficient acceleration of positron rings over tens of centimeters. It is stable

despite the driving beam's evolution for a long period of time owing to the strong focusing fields we have derived analytically. Emittance growth is also limited when the witness beam is properly matched to the wakefield setup.

This work has been funded in parts by DFG (project PU 213/9-1). In the part concerning the analytical model, the work was supported by the Russian Science Foundation (Grant No. 20-12-00077). The authors gratefully acknowledge the Gauss Centre for Supercomputing e.V. (www.gauss-centre.eu) for funding this project (qed20) by providing computing time through the John von Neumann Institute for Computing (NIC) on the GCS Supercomputer JUWELS at Jülich Supercomputing Centre (JSC). L.R. would like to thank X.F. Shen for the helpful discussions throughout this project.

-
- [1] S. Doebert and S. Sicking, *Europhysics News* **49/1**, 24-28 (2018)
 - [2] T. Tajima and J. M. Dawson, *Phys. Rev. Lett.* **43**, 267-70 (1979)
 - [3] A. Pukhov and J Meyer-ter Vehn, *Appl. Phys. B* **74**, 355 (2002)
 - [4] P. Chen et al., *Phys. Rev. Lett.* **54**, 693 (1985)
 - [5] S. P. D. Mangels et al., *Phys. Rev. ST Accel. Beams* **15**, 011302 (2012)
 - [6] M. Zeng et al., *Phys. Plasmas* **21**, 030701 (2014)
 - [7] H. Ekerfelt et al., *Sci. Rep.* **7**, 12229 (2017)
 - [8] J. Faure et al., *Nature* **431**, 541 (2004)
 - [9] B. Hidding et al., *Phys. Rev. Lett.* **108**, 035001 (2012)
 - [10] W. P. Leemans et al., *Nature Phys.* **2**, 696-699 (2006)
 - [11] N. Jain et al., *Phys. Rev. Lett.* **115**, 195001 (2015)
 - [12] S. Corde et al., *Nature* **524**, 442 (2015)
 - [13] S. Gessner et al., *Nat. Commun.* **7**, 11785 (2016)
 - [14] T. Silva et al., *Phys. Rev. Lett.* **127**, 104801 (2021)
 - [15] S. Diederichs et al., *Phys. Rev. Accel. Beams* **22**, 081301 (2019)
 - [16] S. Green et al., *Plasma Phys. Control. Fusion* **56**, 084011 (2014)
 - [17] R. J. Shalloo et al., *Phys. Rev. Accel. Beams* **22**, 041302 (2019)
 - [18] S. Diederichs et al., *Phys. Rev. Accel. Beams* **23**, 121301 (2020)
 - [19] P. Tomassini et al., *Phys. Rev. Accel. Beams* **22**, 111302 (2019)
 - [20] A. Pukhov, *CERN Yellow Reports* **1**, 181 (2016)
 - [21] D. E. Rivas et al., *Sci. Rep.* **7**, 5224 (2017)
 - [22] G.-B. Zhang et al., *Phys. Plasmas* **23**, 033114 (2016)
 - [23] C. Baumann and A. Pukhov, *Phys. Plasmas* **25**, 083114 (2018)
 - [24] A. A. Golovanov et al., *Phys. Plasmas* **24**, 103104 (2017)
 - [25] D. H. Whittum, A. M. Sessler, J. M. Dawson *Phys. Rev. Lett.* **64**, 2511 (1990)
 - [26] J. B. Rosenzweig, B. Breizman, T. Katsouleas, J. J. Su *Phys. Rev. A* **44**, R6189 (1991)
 - [27] W. K. H. Panofsky and W. A. Wenzel, *Rev. Sci. Instrum.* **27**, 967 (1956)